A 1/4°-Spatial-Resolution Daily Sea Surface Temperature Climatology Based on a Blended Satellite and in situ Analysis

VIVA F. BANZON

NOAA/NESDIS/National Climatic Data Center, Asheville, North Carolina

RICHARD W. REYNOLDS

Cooperative Institute for Climate and Satellites, North Carolina State University, Asheville, North Carolina

DIANE STOKES

NOAA/NWS/NCEP/Environmental Modeling Center, College Park, Maryland

YAN XUE

NOAA/NWS/NCEP/Climate Prediction Center, College Park, Maryland

(Manuscript received 22 April 2014, in final form 4 August 2014)

ABSTRACT

A new sea surface temperature (SST) climatological mean was constructed using the first 30 years (1982–2011) of the NOAA daily optimum interpolation (OI) SST. The daily analysis blends in situ and satellite data on a 1/4° (~25 km) spatial grid. Use of an analysis allows computation of a climatological value for all ocean grid points, even those without observations. Comparisons were made with a monthly, 1°-spatial-resolution climatology produced by the National Centers for Environmental Prediction, computed primarily from the NOAA weekly OISST. Both climatologies were found to provide a good representation of major oceanic features and the annual temperature cycle. However, the daily climatology showed tighter gradients along western boundary currents and better resolution along coastlines. The two climatologies differed by over 0.6°C in high-SST-gradient regions because of resolution differences. The two climatologies also differed at very high latitudes, where the sea ice processing differed between the OISST products. In persistently cloudy areas, the new climatology was generally cooler by approximately 0.4°C, probably reflecting differences between the input satellite SSTs to the two analyses. Since the new climatology represents mean conditions at scales that match the daily analysis, it would be more appropriate for computing the corresponding daily anomalies.

1. Introduction

Sea surface temperature (SST) variability is often described as anomalies or departures from normal. If this is not done, the signals of interest may be obscured by the wide ocean temperature range from tropical (>30°C) to polar regions (<0°C) and over the annual cycle. A multiyear average over a base period is defined as the climate normal or climatological mean (CM). The daily SST anomaly is simply the difference between the SST and the CM for the same day. It is important that the temporal and spatial resolution of the CM and the SST be the same. Otherwise, the anomalies will contain resolution differences that may mask the actual temporal and spatial signals.

The World Meteorological Organization (WMO) recommends a standardized approach of computing the CM using the most recent 30-yr period and performing an update at the start of each decade. In compliance, the National Centers for Environmental Prediction (NCEP) recently released a monthly SST climatology on a 1° spatial grid for the 1981–2010 base period (hereinafter referred to as NCEP_CM). (A full description of the NCEP_CM can be found online at http://origin.cpc.ncep.noaa.gov/products/people/yxue/sstclim/.) Briefly,

Corresponding author address: Viva F. Banzon, NOAA/NESDIS/NCDC, 151 Patton Ave., Asheville, NC 28801.
E-mail: viva.banzon@noaa.gov

DOI: 10.1175/JCLI-D-14-00293.1

the NCEP_CM is computed using two SST analyses. The year 1981 is represented by a monthly SST analysis on a 2° spatial grid that uses only in situ data (Smith et al. 2008; Banzon et al. 2010). For the other years (1982–2010), monthly averages of the National Oceanic and Atmospheric Administration (NOAA) weekly optimum interpolation (OI) SST analysis produced by NCEP (referred to as WKOISST in this paper) are used. As described in Reynolds et al. (2002), WKOISST combines in situ and satellite data on a 1° spatial grid using optimum interpolation. For the NCEP_CM, the use of WKOISST started in 1982 because that was the first full year in which multichannel infrared retrievals were available from the Advanced Very High Resolution Radiometer (AVHRR) satellite instruments. The computation follows the Smith and Reynolds (1998) methodology, which had been employed by Xue et al. (2003) for the preceding base period (1971–2000).

Reynolds et al. (2007) developed a higher resolution analysis known as the NOAA daily optimum interpolation SST (hereinafter referred to as DYOISST) that combines in situ and satellite data on a ¼° spatial grid. DYOISST is currently available as version 2 (described in Reynolds 2009) and produced by the National Climatic Data Center. At the time of release, the DYOISST anomalies were computed using the 1971–2000 CM (Xue et al. 2003), bilinearly interpolated in space and time to match the daily ¼° resolution. However, the resulting anomaly patterns were contaminated by artifacts arising from the differing actual resolutions and were not necessarily related to interannual and interdecadal variability. In particular, coastal flows were not well represented in the 1° climatology. Currents, characterized by pronounced SST gradients, could appear weaker or be slightly offset from their actual location when averaged to the 1° grid. The timing of events (i.e., seasonal peak) could also be shifted when interpolating from monthly to daily scales.

The objective of this work is to describe a new ¼° daily climatology (hereinafter DYOI_CM) based only on the DYOISST. Note that there are actually two versions of the daily product. One version uses AVHRR data and is computed from September 1981 to present. The other version adds microwave satellite data but spans a shorter period (2002–11). In this paper, DYOISST refers to the daily OI version using AVHRR only. Since AVHRR data cover only part of 1981, the base period selected is 1982–2011, which is shifted by one year compared to the WMO-compliant NCEP_CM. Aside from the ability to resolve submonthly to daily scales, the expected advantages of the DYOI_CM would be better-defined SST gradients, better resolution along the coast, and a more suitable climatology for computing DYOISST anomalies. Certainly, a purely satellite SST climatology can also be made, but an analysis provides additional information for areas not well covered by AVHRR, such as ice margins and cloudy regions.

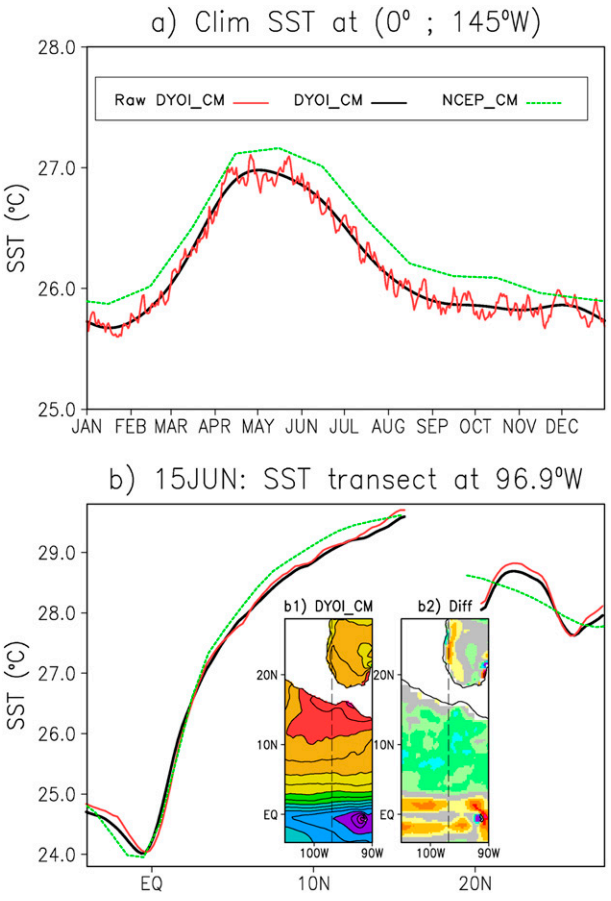

FIG. 1. (a) Unfiltered (red line) and temporally smoothed (black line) DYOI_CM at center of the Niño-3.4 region (0°, 145°W). Green dashed line shows the NCEP_CM is up to 0.2°C warmer at this grid point. (b) The same three climatological means, but along a meridional section (4°S–28°N) on 15 June crossing a river plume at ~26°N and the equatorial cold tongue between ~4°S and 4°N. Inset b1 is a map of the smoothed DYOI_CM (0.5 C° contour intervals). Inset b2 is the boxed area from Fig. 3b that should also be referred to for color scale. Vertical dotted line in both insets of (b) shows transect location.

In the remaining part of the paper, the methodology to construct the DYOI_CM is described. This is followed by the results, where the DYOI_CM is compared to the NCEP_CM, and a final summary (the DYOI_CM is available online at ftp://eclipse.ncdc.noaa.gov/pub/OI-daily-v2/climatology/).

2. Data and methods

As mentioned previously, DYOISST refers to the analysis that uses only AVHRR satellite SSTs (Reynolds

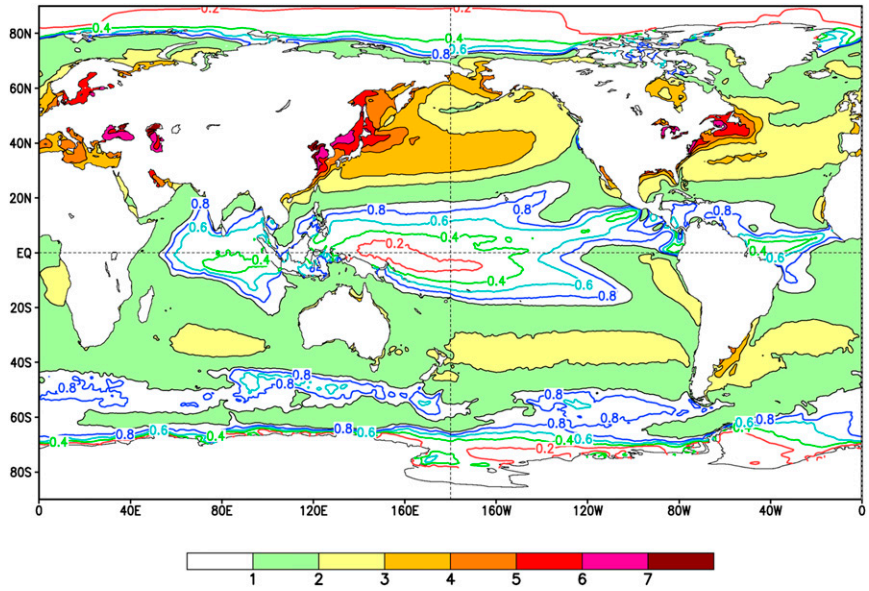

FIG. 2. Standard deviation of the DYOI_CM. Shading is shown for standard deviations of 1°C and above. Labeled contours are shown for 0.2°, 0.4°, 0.6°, and 0.8°C.

et al. 2007), currently available as version 2 (www.ncdc.noaa.gov/sst/griddata.php). DYOISST data were averaged over 30 years (1982–2011) to obtain the mean and standard deviation at each ¼° spatial grid point for each of the 365 days (one year). The analyses for 29 February (occurring in 7 leap years out of the 30 years) were not used. This simple average is referred to as the raw or unfiltered DYOI_CM. Because the result tended to contain day-to-day observational noise (Fig. 1a), smoothing was performed. An unsmoothed climatology would have the undesirable effect of producing noisy DYOISST anomalies. Spatially, the individual SST fields were already quite smooth (Fig. 1b) and so no additional filtering was done.

To temporally smooth the raw CM, Fourier components were computed. The frequencies of the components were proportional to one cycle per year multiplied by the number of modes n, where n was an integer ranging from 1 to 182 (i.e., 365/2 − 1). The number of modes was determined by examining the added variance (and standard deviation) explained by each mode. About 99% of the total variability was explained by modes 1–6, that is, 88.1%, 9.2%, 1.0%, 0.3%, 0.3%, and 0.2%, respectively. The number of modes was not increased above 6 since the regions that would benefit (between 10°S and 10°N and north of 80°N) were characterized by low standard deviations (Fig. 2), and therefore the actual added signal would be very small. The same number of modes was used for all grid points for consistency and to avoid creating discontinuities.

The mean and first six Fourier harmonics were used to generate a filtered daily mean, henceforth DYOI_CM. Using only six harmonics should give monthly averaged variability similar to that occurring in other CM monthly products (e.g., NCEP_CM). The DYOI_CM has a smoother temporal progression compared to the NCEP_CM (Fig. 1a) that had been bilinearly interpolated to produce daily values. To account for leap years, a DYOI_CM field for 29 February was computed by averaging the DYOI_CM fields for 28 February and 1 March. Thus, for each day, the DYOI_CM value is always the same for both leap and nonleap years.

It should be noted that the DYOI_CM standard deviation (Fig. 2) is visually identical to the unfiltered version (not shown) because the filtered higher frequencies have very small contributions to the standard deviation. As expected, standard deviation is low in the tropics, especially in the western Pacific, and near seasonal sea ice areas. The highest standard deviation occurs in northern midlatitudes, particularly along western boundary currents. The next largest variability is primarily in southern midlatitudes.

3. Results

The new DYOI_CM was quite similar to the NCEP_CM, with differences generally below 0.5°C except at specific locations, that is, areas with strong currents or pronounced upwelling (Fig. 3). During the boreal winter, these along-current differences were

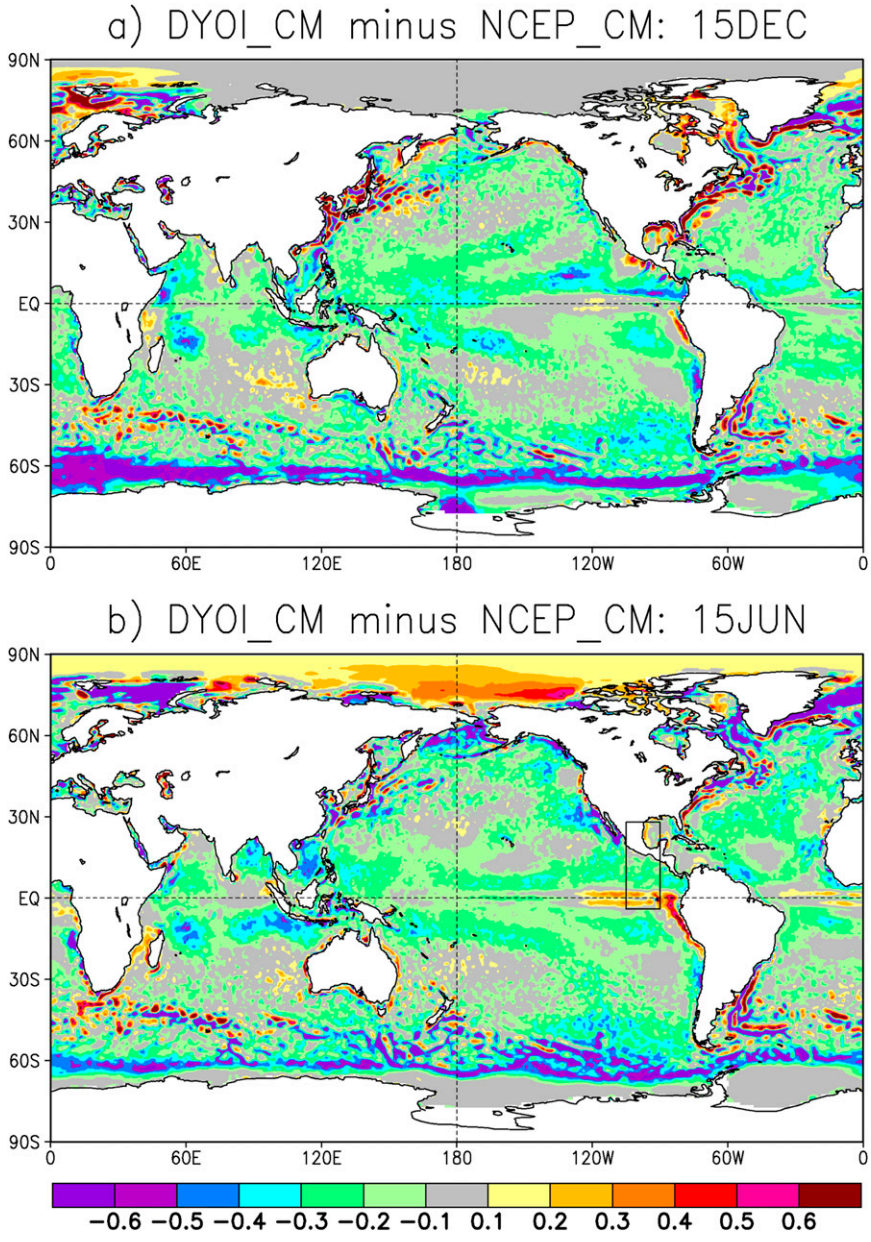

FIG. 3. Difference between the daily OISST and NCEP climatologies in boreal (a) winter and (b) summer. Box in (b) shows area enlarged in Fig. 1b, inset b2.

stronger in the Northern Hemisphere currents (e.g., along the Kuroshio, Gulf Stream, and Greenland and Labrador Currents) than in the Southern Hemisphere currents (e.g., the Antarctic Circumpolar and Falkland/Malvinas Currents) (Fig. 3a). The reverse occurred in boreal summer (Fig. 3b). Note in particular that where variability is greatest along these highly dynamic features (e.g., along 50° and 60°S), the differences tended to alternate between positive and negative values, reflecting the ability of the higher-resolution climatology to resolve smaller scales better than the NCEP_CM. A similar situation occurred in the Gulf of Mexico (Fig. 1b, inset b2), where coastal riverine outflow was cooler than the Gulf waters. In the SST section between 20° and 28°N, the DYOI_CM shows a local maximum and minimum, while the NCEP_CM decreases almost monotonically (Fig. 1b). The ability to resolve the finer features stems from the spatial correlation scales used for DYOISST, which are much smaller than those for WKOISST (Reynolds et al. 2007).

TABLE 1. Input datasets used in the weekly and daily OISST. Explanation of acronyms and other details are not provided here for brevity but can be found in Reynolds et al. (2002, 2007).

OISST product	1° weekly OISST version 2	1/4° daily OISST version 2
Release date	November 2001	November 2008
Reference	Reynolds et al. (2002)	Reynolds et al. (2007); Reynolds (2009)
AVHRR SSTs	• 1981–89: University of Miami weekly SST fields computed from operational National Environmental Satellite, Data, and Information Service (NESDIS) SSTs • 1990–95: operational NESDIS daily SSTs • 1996–present: operational U.S. Navy daily SSTs	• 1981–85: Pathfinder version 5.1 • 1985–2006: Pathfinder version 5.0 • 2007–present: operational U.S. Navy daily SSTs; 2 AVHRRs used
Buoy and ship SSTs	• 1981–97: Comprehensive Ocean–Atmosphere Data Set (COADS) release 2 • 1997–present: operational daily NCEP Global Telecommunication System (GTS) data	• 1981–2006: International COADS (ICOADS) 2.4 • 2007–present: Operational daily NCEP GTS data
Sea ice concentrations (for proxy SSTs at ice edge)	• 1981–99: Homogenized ice fields based on 4 analyses including National Aeronautics and Space Administration (NASA) Goddard Space Flight Center (GSFC) team and operational NCEP ice analysis • Late 1999–present: Operational NCEP ice analysis	• 1981–2004: NASA GSFC team algorithm • 2005–present: Operational NCEP ice analysis

This is also related to the curious difference pattern observed in the eastern tropical Pacific in boreal summer, where along either side of the equator, there is a strong positive difference (>0.2°C) between the two climatologies (Fig. 3b; close-up in Fig. 1b, inset b2). The transect between 4°S and 0° illustrates how the pattern is formed (Fig. 1b). While both CM values are similar at the equator, the DYOI_CM warms faster going southward. The net effect is that the DYOI_CM defines a narrower cold tongue with a minimum closer to the equator compared to the NCEP_CM. In winter (Fig. 3a), the difference pattern was generally absent since the region was relatively cooler and the SST gradients were not as sharp.

Differences between the two climatologies were also notable in the near-polar regions, especially in the Arctic (Fig. 3). This indicated a difference in the proxy SSTs computed from sea ice concentrations for the two OISST products. The sea ice concentration datasets used in the WKOISST and the DYOIST are not the same (Table 1). For the early years, the ice input to the WKOISST is a homogenized product based on four datasets and bias adjusted to be consistent with historic in situ ice data, as described in Reynolds et al. (2002). In contrast, the DYOISST uses only one ice dataset and therefore is not bias adjusted (Reynolds et al. 2007). For forward processing, both analyses use the same ice data from NCEP, but WKOISST started using NCEP ice from 1999 onward while DYOISST, developed later, uses these ice data only after 2004. Because in situ data in these regions are very sparse, it is not clear which CM is more correct.

A smaller but more spatially widespread difference (~0.4°C) is also evident (Fig. 3). The DYOI_CM was systematically cooler than the NCEP_CM at locations of persistent cloud cover, such as the ITCZ, and along seasonal dust plume trajectories. The pattern changed with season as the global distribution of clouds and dust aerosols shifted. This small difference is most likely due to the use of operational (i.e., near–real time) SSTs in WKOISST and AVHRR Pathfinder SSTs (version 5.0/5.1) in DYOISST (Table 1). Operational SSTs tend to be warmer relative to an in situ–only analysis, while Pathfinder SSTs tend to be cooler, possibly because of cloud contamination (Reynolds et al. 2007), but many other processing differences exist (Kilpatrick et al. 2001). Relative to buoys, the reported Pathfinder bias is minimal: 0.02° ± 0.5°C (Kilpatrick et al. 2001), while operational SSTs have <0.1°C monthly bias error and <0.6°C root-mean-standard error (May et al. 1998). Thus, satellite retrieval uncertainty is comparable to the differences reported here. These statistics are based on buoys that are not error-free. For example, depending on manufacturer, type, and time of day, oceanic drifters have a wide range of biases (from −0.03° to 0.61°C) and standard deviations (from 0.48° to 0.61°C) relative to AVHRR SSTs (Castro et al. 2012). If satellite error is accounted for, O'Carroll et al. (2012) estimated the global drifter standard deviation is approximately 0.2°C. It should also be noted that other SST analyses have similar biases (Reynolds and Chelton 2010).

Even though both the DYOISST and WKOISST methodologies include a step that uses in situ data to

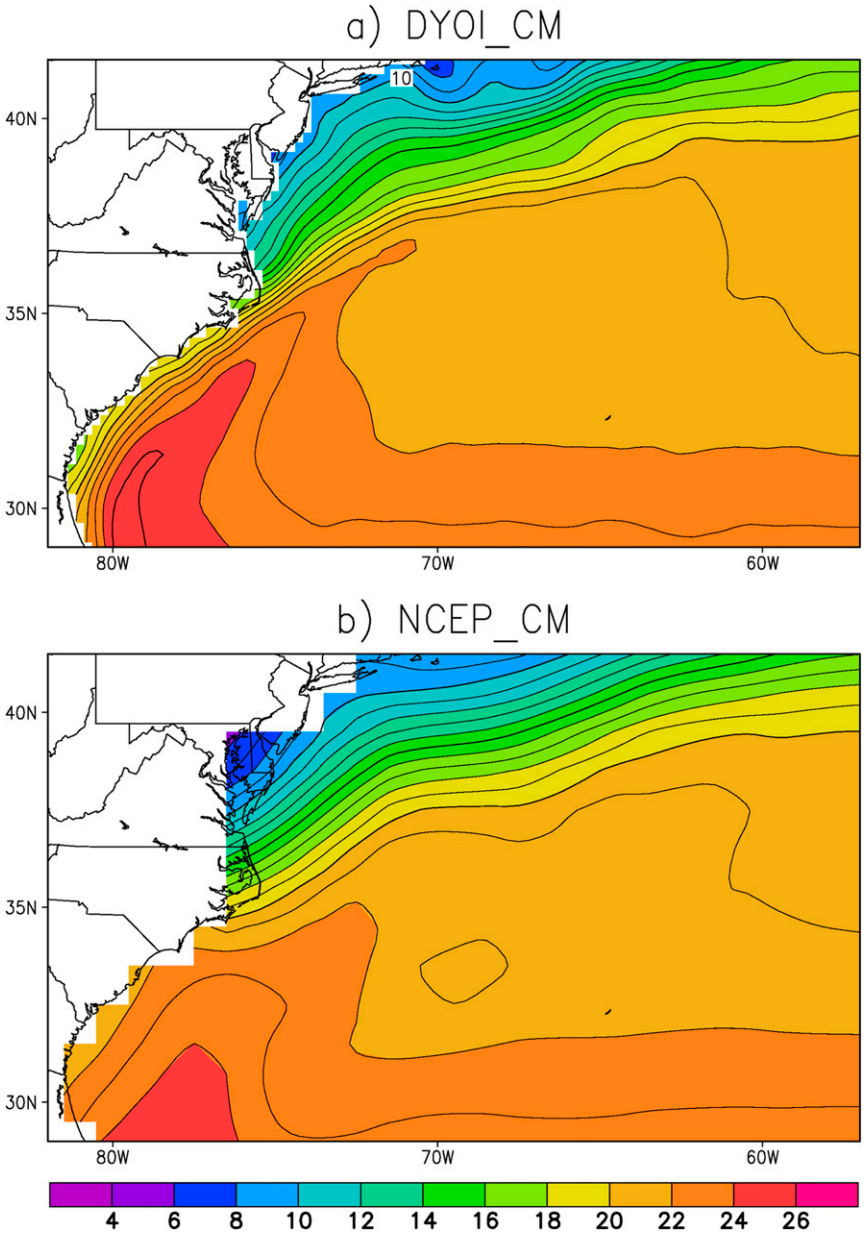

FIG. 4. SSTs (°C) for 15 Dec along the U.S. East Coast as represented by (a) the DYOI_CM and (b) the NCEP_CM. Color shading interval is 2°C (see color scale). Contour line interval is 1°C.

correct satellite biases, residual amounts remain in both OISST products, leading to the CM difference. It would have been desirable to use the same AVHRR product for the entire production period for both analyses. However, that was not possible as some of the early operational AVHRR SSTs were lost. Unfortunately, the Pathfinder dataset is not updated in real time. Other differences between the two OISST methodologies, such as bias correction, are discussed in Reynolds et al. (2007). In the current DYOISST version 2, 0.14°C is subtracted from ship SSTs to account for differences relative to buoy SSTs (Reynolds 2009). This adjustment is not in the WKOISST because, at the time of the WKOISST version 2 release, ship observations were more common than buoy measurements (e.g., see Fig. 2 in Reynolds et al. 2002).

In terms of the annual cycle, the amplitude and phase were similar between the DYOI_CM and NCEP_CM, as shown in the Niño-3.4 region (Fig. 1a). For reasons already discussed, the DYOI_CM was cooler than the NCEP_CM by about 0.2°C all year at this location. The offset was about the same for the areal average, that is,

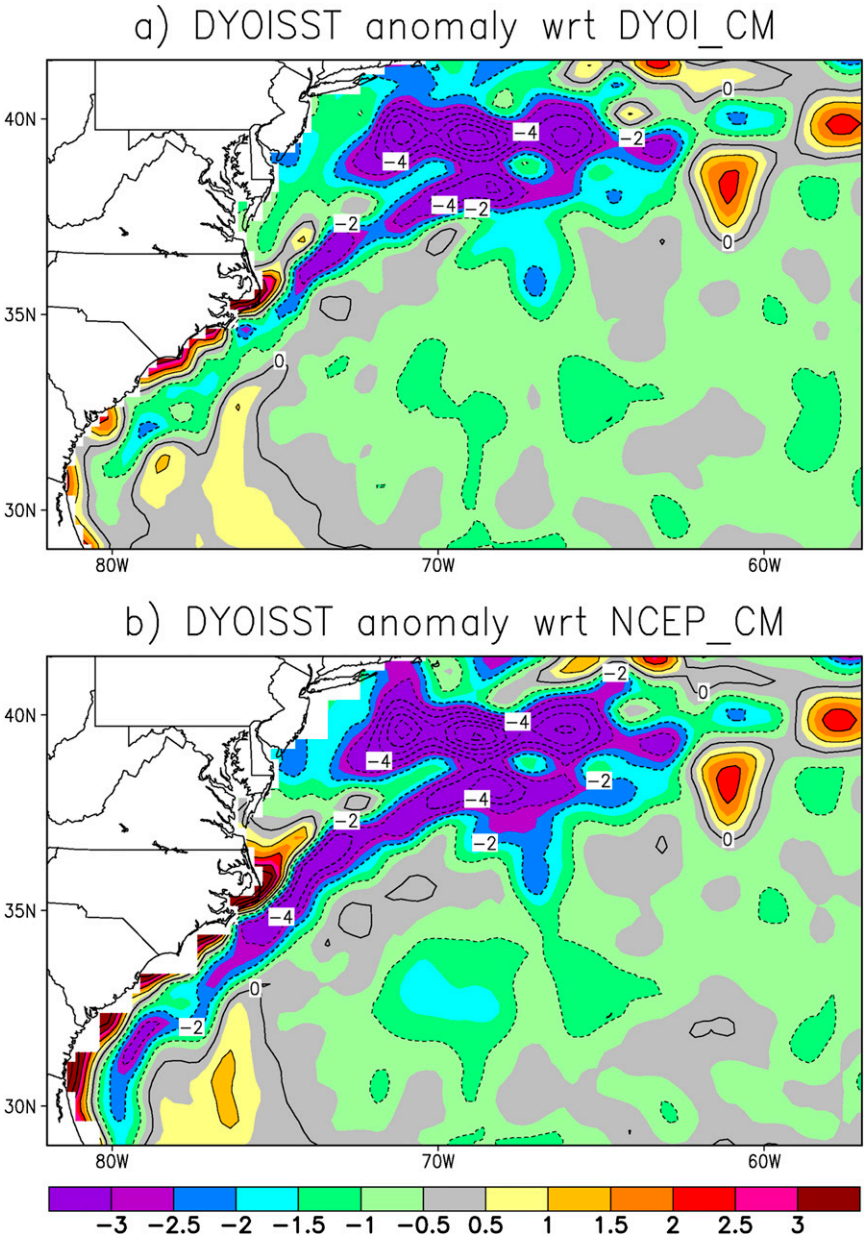

FIG. 5. DYOISST anomaly field (°C) for 15 Dec 2011 along the U.S. East Coast computed with respect to (a) the DYOI_CM and (b) the NCEP_CM, both shown in Fig. 4. Color shading interval is 0.5°C (see color scale). Contour line interval is 1°C.

the Niño-3.4 index. For brevity, other Niño regions are not shown here, but it should be noted that the offsets are very dependent on location. For example, the cool bias is pronounced all year in the Niño-4 region but is slight in the Niño-3 region. In the Niño-1 region, the DYOI_CM was actually slightly warmer part of the year. Although these offsets are actually not very large, they have to be taken into consideration for some applications. For example, since El Niño/La Niña detection is based on whether anomalies fall outside the range from −0.5° to 0.5°C, the behavior of the anomalies during past major events and the SST uncertainty should be taken into account.

The two climatologies can be visually compared in a close-up of the Gulf Stream region. In Fig. 4, the DYOI_CM shows the Gulf Stream SST gradient with tighter isotherms at some locations than the NCEP_CM. Also, there is a stronger cool flow along the southeastern U.S. coast in the DYOI_CM, contrasting with the warmer offshore water. The NCEP_CM shows a homogeneous gradient across the Gulf Stream. The coastal

flow off Georgia and the Carolinas is weak and the water is not as cold. Thus, the DYOISST anomalies computed using the NCEP_CM tended to still contain the mean coastal flow compared to those computed with respect to DYOI_CM (Fig. 5). As expected, the NCEP_CM was effective in removing the larger-scale mean features, but not those at the finer scales analyzed in the DYOISST.

4. Conclusions

Both the DYOI_CM and NCEP_CM provide a good representation of global SSTs. However, the new DYOI_CM is a better match to the spatial and temporal scales of the DYOISST, especially near western boundary currents and along the coast, and is therefore better suited to compute DYOISST anomalies. In addition to these resolution-related differences, the two climatologies were not in exact agreement at specific locations, primarily because of differences in input satellite SST datasets used in the WKOISST (which uses operational SSTs) and DYOISST (which is mostly based on AVHRR Pathfinder SSTs). However, the differences were within the limits of satellite SST retrieval error and comparable to biases in other analyses. Disparities between the two climatologies near the poles may be caused by differing sea ice inputs and processing between the two analyses. If the two OISSTs were reprocessed using the same inputs, these overall bias differences would be minimized. Users need to be aware of these caveats associated with using anomaly fields.

Acknowledgments. The graphics were generated using Grid Analysis and Display System (GrADS), made publicly available at http://grads.iges.org/grads by the Center for Ocean–Land–Atmosphere Studies.

REFERENCES

Banzon, V. F., R. W. Reynolds, and T. M. Smith, 2010: The role of satellite data in extended reconstruction of sea surface temperatures. *Proc. "Oceans from Space" Symp.,* Venice, Italy, Joint Research Center, European Commission, 27–28, doi:10.2788/8394.

Castro, S. L., G. A. Wick, and W. J. Emery, 2012: Evaluation of the relative performance of sea surface temperature measurements from different types of drifting and moored buoys using satellite-derived reference products. *J. Geophys. Res.,* **117,** C02029, doi:10.1029/2011JC007472.

Kilpatrick, K. A., G. P. Podesta, and R. Evans, 2001: Overview of the NOAA/NASA Advanced Very High Resolution Radiometer Pathfinder algorithm for sea surface temperature and associated matchup database. *J. Geophys. Res.,* **106,** 9179–9198, doi:10.1029/1999JC000065.

May, D. A., M. M. Parmeter, D. S. Olszewski, and B. D. McKenzie, 1998: Operational processing of satellite surface temperature retrievals at the Naval Oceanographic Office. *Bull. Amer. Meteor. Soc.,* **79,** 397–407, doi:10.1175/1520-0477(1998)079<0397:OPOSSS>2.0.CO;2.

O'Carroll, A. G., T. August, P. Le Borgne, and A. Marsouin, 2012: The accuracy of SST retrievals from Metop-A IASI and AVHRR using EUMETSAT OSI-SAF matchup dataset. *Remote Sens. Environ.,* **126,** 184–194, doi:10.1016/j.rse.2012.08.006.

Reynolds, R. W., 2009: What's new in version 2. OISST web page, NOAA/NCDC. [Available online at www.ncdc.noaa.gov/sst/papers/oisst_daily_v02r00_version2-features.pdf.]

——, and D. B. Chelton, 2010: Comparisons of daily sea surface temperature analyses for 2007–08. *J. Climate,* **23,** 3545–3562, doi:10.1175/2010JCLI3294.1.

——, N. A. Rayner, T. M. Smith, D. C. Stokes, and W. Wang, 2002: An improved in situ and satellite SST analysis for climate. *J. Climate,* **15,** 1609–1625, doi:10.1175/1520-0442(2002)015<1609:AIISAS>2.0.CO;2.

——, T. M. Smith, C. Liu, D. B. Chelton, K. S. Casey, and M. G. Schlax, 2007: Daily high-resolution blended analyses for sea surface temperature. *J. Climate,* **20,** 5473–5496, doi:10.1175/2007JCLI1824.1.

Smith, T. M., and R. W. Reynolds, 1998: A high resolution global sea surface temperature climatology for the 1961–90 base period. *J. Climate,* **11,** 3320–3323, doi:10.1175/1520-0442(1998)011<3320:AHRGSS>2.0.CO;2.

——, ——, T. C. Peterson, and J. Lawrimore, 2008: Improvements to NOAA's historical merged land–ocean surface temperature analysis (1880–2006). *J. Climate,* **21,** 2283–2296, doi:10.1175/2007JCLI2100.1.

Xue, Y., T. M. Smith, and R. W. Reynolds, 2003: Interdecadal changes of 30-yr SST normals during 1871–2000. *J. Climate,* **16,** 1601–1612, doi:10.1175/1520-0442-16.10.1601.